FATIGUE OF SMALL REINFORCED CONCRETE BEAMS WITH END-ANCHORED REINFORCEMENT

by

ABOLFAZL NOORY-KOOPAEE

B.S.C.E., Kansas State University, 1978

A MASTER'S REPORT

submitted in partial fulfillment of the

requirements for the degree

MASTER OF SCIENCE

Department of Civil Engineering

Kansas State University

Manhattan, Kansas

1978

Approved by:

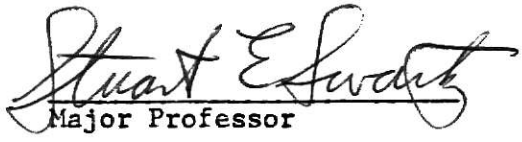

Major Professor

TABLE OF CONTENTS

THIS BOOK CONTAINS NUMEROUS PAGES WITH DIAGRAMS THAT ARE CROOKED COMPARED TO THE REST OF THE INFORMATION ON THE PAGE.

THIS IS AS RECEIVED FROM CUSTOMER.

LIST OF TABLES AND FIGURES

CHAPTER I - INTRODUCTION

The utilization of reinforced concrete in structural applications continues to increase; for this reason many different kinds of studies have been done on this material.

In the area of fatigue studies on reinforced concrete relatively little work has been done in comparison to other areas of study.

This report describes experiments on reinforced concrete beams subjected to cyclic loads.

The main purposes of the research reported herein can be tabulated as follows:

1. Observe crack growth $\underline{V}$ cycles in specimens where bond failure and failure of steel reinforcing is prevented.

2. Observe the mode of failure in beams with different depth to span ratios.

3. Evaluate the effectiveness of the photoelastic coating technique to monitor cracking in concrete.

The tests were carried out on eight reinforced concrete beams of rectangular cross section.

The type of loading, length, shape of the cross section and type of reinforcing bar in all nine beams were the same, but the size of the reinforcing bars and the cross section were varied. These parameters appear to have a strong influence on the fatigue life of the concrete.

The following factors were considered for designing the beams:

1. Beams designed using cracked-section working stress theory.

2. The reinforcing was anchored with end plates so potential bond failure was not considered a parameter.

3. The maximum stress level in the steel was 1/3 to 1/2 f_y while the maximum stress level in the concrete was approximately 1/2 f'_c.

The methods, results and conclusions of past experiments on related topics have been reviewed and a summary is given in the next section.

The chapter on the testing program considers the design of specimens. A short discussion of the photoelastic coating technique, how it works, how the specimen's surface should be prepared and, in general, what needs to be done is also given in this chapter. This chapter also contains the test procedure, how to use the facilities and the important factors that need to be considered when operating the machine.

The information collected from the tests which describe the behavior of the beams under the cyclic loads is given in the chapter on experimental results.

Finally, a summary of this work with conclusions and design recommendations is given.

CHAPTER II - LITERATURE SURVEY

The publications dealing with fatigue aspects of reinforced concrete under cyclic loads are rather limited.

A test on strength and deformation characteristics of plain concrete was done by Award and Hilsdorf (1); in this test 300 concrete prisms were subjected to static and dynamic loads. The dynamic load range was 80-95% of the static compressive strength.

Raithby and Galloway (6) have investigated the effects of moisture condition, age and rate of loading on the fatigue of plain concrete beams. Their specimens were cured under water before testing and ranged in age prior to testing from 28 days to 3 years. In these tests a constant cyclic load was applied and the maximum and minimum loads were controlled in each cycle.

A fatigue test on composite bridge slabs was done by Dev Batchelor and Hewitt (3) which also considered the economic problems associated with design. Their work showed that slabs designed by economical methods behave well under the action of cyclic loads.

Consideration for design of concrete structures subjected to fatigue loading was reported by ACI Committee 215 (2). This report concluded that locations of stress concentrations in steel reinforcement, such as at tendon anchorage and bond in reinforcement are critical. In general, the stress range, which is the difference between the minimum and maximum stress, is most critical for fatigue.

Shah and Chandra (7) have investigated the mechanics of failure of paste and concrete subjected to cyclic or sustained stresses. Maximum cyclic sustained stresses of 60-90% of the short-term compressive strength

were applied. They concluded that in this range, increasing the number of cycles to failure will decrease the strength of the concrete.

Walls, Sanders and Munse (10) ran an experimental and analytical study of "Fatigue Behavior of Butt-welded Reinforcing Bars in Reinforced Concrete Beams". Their work shows that the stress in the bar tends to increase slightly as the number of cycles increase for constant applied fatigue loads. This is due to propagation of the concrete crack caused by the reduction of tensile strength of concrete under cyclic load.

Venuti (9) in a study of fatigue failure analysis, analyzed 106 beam specimens with steam curing at 160° F for 16 hours. A group of two beams survived 5,000,000 cycles and seven failed in fatigue at cycles of loading varying from 464,900 to 3,195,000. A group of 16 beams were tested under static loads for determination of ultimate strength. In 14 of those, the mode of failure was the same, and was due to excessive elongation of the steel bars.

A research report has been done by Ople and Huisbos (5) on fatigue life of plain concrete. Tests were conducted with a frequency of 500 cycles per minute. The maximum and minimum loads were applied until failure or 2,000,000 cycles, whichever occurred first.

A change in stress of only 7.5 percent caused the fatigue life to change from approximately 40,000 to 1,000,000 cycles.

The results presented by Swartz, Hu, Jones (8) on tests of pre-cracked concrete indicate that the failure mechanism does not depend on particle size and is a combination of bond failure and aggregate fracture. They also concluded that crack growth can be controlled during the fatigue process.

The conclusions of the past experiments can be tabulated as follows:

1. The number of cycles to failure will increase by decreasing the stress range. (1)

2. Damage of the concrete is both time dependent and the cycle dependent, i.e., (1)

$$D_n = \frac{n'}{n_o} \quad , \quad D_t = \frac{t}{t_u}$$

D_n = cycle dependent damage

n' = number of applied cycles

n_o = number of cycles to failure under pure fatigue condition

D_t = time dependent damage with a sustain load

t = duration of loading under constant stress level, σ

t_u = load-time to failure under the same stress level, σ

3. After 30-70 percent of the number of cycles to failure, increasing the number of cycles, will decrease the strength of the concrete. (1)

4. An increase in the number of cycles will increase the width of the crack. (10)

5. At high stresses, the number of cycles has a significant effect on the fatigue life of concrete. (1)

6. After the cracks appear in the concrete, they will start to grow and almost no new crack will form. (10)

7. In the slabs, first the initial deflection will increase, then it will stay constant. (3)

8. The fatigue life of concrete is directly proportional to the age of the concrete. (6)

9. Effect of moisutre has a critical influence on the fatigue life of concrete. (6)

10. The crack generally will not go through the aggregate particles, but rather the bond between the mortar and the aggregate will be lost. (7)

11. As the load is repeated, flexural tensile cracks will migrate toward the top of the beam. (7)

12. Crack progression may go up to several million cycles at low load levels. (5)

13. A small change in the maximum stress level has a large effect on concrete fatigue life. (5)

14. The equation of

$$Q = 1 - (1-P)^{u_1}$$

is a good estimate of the probability to failure between the concrete beam section and the test specimen.

Q = probability of the prototype beam to fail at or before N cycles

P = the corresponding probability of small test specimen failure

u_1 = the ratio of width of the prototype beam to the width of the test specimen

15. The age of the concrete at testing has a great influence on deflection. Sudden substantial increase in crack widths and deflection took place only at the final fatigue failure. (6)

CHAPTER III - TESTING PROGRAM

A. Introduction

All beam tests were made such that the existing facilities could be used and were conducted on a materials testing system machine (MTS Model 903.32).

A total of eight beams were made with two different types of design. They all were simply-supported on steel rollers. The load was applied in a vertical direction to the middle of the top surface of the test specimen through another steel roller. A drawing of the test set-up for one type of beam is given in Fig. 1.

The test program was divided into two phases. In phase one the ratio of depth to span was high relative to that used in phase two.

The length of the beams and the material properties of the concrete were the same for all eight beams.

The beams were subjected to repeated loads with a frequency maintained at approximately 250 cycles per minute, or 4 hertz.

B. Description of Test Specimens

Complete dimensions of both types of beam specimens are given in Figs. 2 and 3.

The aggregate was well-graded with a specific gravity of 2.5 and was 3/8 in. minus. The sand had a specific gravity of 2.49. Type 3 cement was used with a water-cement ratio of 0.8.

Also in addition to the beams, several 3 in. x 6 in. cylinders were made and tested in direct compression in order to find out the strength of the concrete. These were tested after seven days in water and seven days air-dried. The results of these tests are given in Table 1.

The yield point of the steel was 48.82 ksi for the No. 2 bars and 61.93 ksi for the No. 5 bars.

The size of the steel bar was established on the basis of the strength of both steel and concrete. The pertinent calculations are given in Appendix I.

For type one, two No. 5 bars were used with a total cross-sectional area of 0.61 in.^{2} (3.81 cm^2); three No. 2 bars with a total cross-sectional area of 0.147 in.^{2} (0.92 cm^2) were used in the type two beams.

The loads to be applied were based on initial calculations with the requirement that the maximum concrete stress was about 0.5 f'_c. These maximum loads were about 5 kips (22240 dynes) and 600 lb. (2668.8 dynes) were estimated for type one and two beams, respectively. These calculations are given in Appendix I.

The maximum load and load range for each beam are given in Table 2. Also given in Table 2 are the maximum concrete and steel stresses and stress ranges.

C. Photoelastic Coating Method

The experimental method of photoelasticity (11) is a method of determination of strains in a model with the aid of polarized light.

In this method, strain patterns are obtained directly from the surface boundary of an applied photoelastic coating and give a complete picture of the maximum strain distribution within the interior for thin specimens.

The change of the optical characteristic which is directly proportional to the change in stress can be observed by using a polariscope.

The polariscope can be arranged in different ways. The arrangement of different parts of reflection polariscope is shown in Fig. (4). The

error introduced by this arrangement is negligible.

The center to center distance between the analyzer and polarizer is about 5 inches and the instrument is about 2 feet from the photoelastic coating which is applied to the beam and which produces the fringe pattern.

The intensity of light as a function of time can be expressed as

$$y = x \sin wt.$$

y = intensity of light (amplitude) at any time

x = maximum intensity

w = the circular frequency of the radiation.

Color is associated with the frequency (w). Hence, monochromatic light is the light of a single frequency (w), whereas white light is a mixture of radiation of various frequencies.

The light which originates at a point is well distributed in all directions as a divergent sphere, so a lens is used to collimate the light. That is, to convert spherically divergent light to parallel rays which will not distribute as divergence or convergence. Likewise, a lens may be employed to focus collimated light to a point (Fig. 5) when a ray of light enters a doubly refracting material at normal incidence (perpendicular to the surface). It is resolved into two plane-polarized, component rays which are transmitted on planes at right angles to each other.

The two rays travel through the material with different velocities and have a slight phase shift relative to one another.

When the two rays reach the analyzer, their components, parallel to the transmission axis of the analyzer, pass through; the others will be stopped. If the phase difference of the two horizontal components is zero or an integral number of the wave length, the two waves cancel to give darkness. On the other hand, if the phase difference is one-half,

three-halves, etc., wave length, the two add to produce maximum intensity. If the phase difference is some intermediate value, the intensity will be somewhere between the two cited extremes.

Selection and Application of Photoelastic Material

One of the important factors for our purpose in selecting the material is the stability in long terms under both static and dynamic load.

Several of the most desired properties can be written as: 1) transparency, 2) suitable value of stress-optical coefficient (K), 3) suitable elastic properties.

Since the coefficient of sensitivity varies linearly with coating thickness,

$$C_c = \frac{2H_c}{F_\varepsilon} \text{ ---------- (1)}$$

the coating sensitivity and the thickness effect must be weighted for choosing the thickness of coating (11).

Temperature is another important factor that must be considered. Because the (K) value is very dependent on the temperature, the environment should be carefully controlled. "The selection of very thin coating (less than 0.02 in. or 0.05 mm.) is not recommended for precise stress analysis since the relative error introduced by variation in thickness from point to point can become excessive" (11).

After the coating is selected, very careful attention should be given to its application because the successful use of this method mainly depends on a perfect bond between the coating and the specimen. The directions given by the manufacturer of the coating describing surface preparation should be followed carefully, then the coating area should be marked and bonded. The cement will be spread over this area and the sheet of coating will be applied as follows.

First, the coating sheet will be placed down at one edge and slowly rotated, then pressed into position. Curing will take place at room temperature over a 24 hour period with a constant pressure.

The thickness of the coating that we used was between .115 ± .002 in. and had a k factor of 0.13 with an f value of 760.

Selection of Adhesive

Since an excellent adhesive bond between the coating and beam is necessary, the selecting, mixing and application of the cement becomes important.

Therefore, every careful thought should be given to the following properties of the cement:

1. Long pot life, to have enough time for application;
2. Low viscosity, to let the extra adhesive flow under the applied coating sheet;
3. Modulus of elasticity should be at least equal to that of coating sheet;
4. Sufficient strain capability to transmit strain up to maximum elongation of the coating;
5. Short curing time;
6. Uniform and high reflectivity.

In the preparation of cement, the amount of cement needed should be calculated in advance. A quantity of one gram of mixed cement will be sufficient for each 1.5 sq-in. (9.675 sq-cm.) of area.

Cement should not be prepared until the surface has been properly prepared and the plastic is ready to bond.

Surface Preparation

The following factors should be considered for a good bond between

the test part surface and the photoelastic plastic coating:

1. Clear the surface from all foreign matter and smooth surface with disc sander, grinder, etc.

2. Clean surface by removing all dust and residue with gauze saturated with alcohol, acetone, etc; this process should be done several times.

3. After surface gets dry, apply adhesive; fill in open pores.

D. Test Procedure

Tests were conducted using a closed-loop, electrohydraulic material testing system (M.T.S.).

For using the MTS machine, the following steps are:

1. Power on Sequence
   a. Put the power switch on.
   b. Put the pump control on local and start the machine, then remove the pump control from local to remote control.
   c. Switch on the hydraulic pump at low pressure.
   d. Adjust set point, generally between 250-350.
2. Warm-up Sequence
   a. Set point on 400-500.
   b. Span on zero.
   c. Select XDCR1 (stroke) for FDBK low load range.
   d. Put the program on, increase the span and let the machine run about one-half hour. At this point temperature should be about 105°F.
   e. Stop the machine by putting span on zero, hydraulic off, then set up the test specimen as it shows in Fig. 1 (the

load applied exactly on the middle of top surface of the beam and one-half inch overhang on each support).

The zero should be checked each time before the test is run.

The following statements should be considered when using the MTS machine:

1. The position of the switches should not change when pressure is applied.

2. The area around the actuator piston rod must be clear so the piston is free to stroke without contacting anything.

3. Because of different reasons, it is possible that the dynamic peaks exceed the programmed operating range, so the set point and the span must be checked to insure that the program peak does not exceed the range.

4. Pictures can be taken under both static and dynamic loads.

5. The frequencies can be increased or decreased when the test is running.

A dial gage was placed on the corner of each specimen to check the deflection with respect to the number of cycles.

The sine function was used to apply load at a constant rate to failure.

Pictures were taken under the maximum static load at various number of cycles as the crack was growing.

CHAPTER IV - EXPERIMENTAL RESULTS

A total of six beams of the first type were tested to failure under fatigue loading. Cracks were observed in all of the beams after several cycles of loading. During the first several hundred cycles, the cracks spread and widened until a relatively stable condition was reached.

The first three beams failed due to a lack of good bond between the steel bars and the end plates (the welded connection failed), but beams No. 5 and 6 did not fail even though the bond between steel and concrete was broken over the entire length between the anchorages. These members cracked and acted as a tied arch as shown in Fig. (6).

Some cracks progressed through the aggregate particles, but the loss of adhesion between the mortar and aggregate was more significant.

Tests were conducted at a rate of 4 Hz with the number of cycles to failure varying from 93,000 to 389,000.

After the cracks reached the top surface on beams No. 5 and 6, the beam still could handle the maximum load but this was carried only by the steel, and sections of concrete were held together by the steel bars and end plates. The mode of failure for this type of beam is shown in Fig. (6).

For the type two design initially the vertical cracks were equally spaced, as shown in Fig. (7).

These cracks progressed through the beam in proportion to the number of load cycles until they finally penetrated through the compressed area and the beam failed. Beam No. 7 failed at 4,830,411 cycles, without any damage to the reinforcing steel bars other than bending which occurred as a result of dowel action after the concrete failed (Fig. 8). New cracks developed as the cycles increased. The position of the cracks for different numbers of cycles and constant load are given in Fig. (9) through (15) for Beam No. 7.

These photographs were used to determine the change in crack depth and width for increasing number of load cycles. The maximum ratio of crack depth to total depth of the beam at different numbers of load cycles was calculated to observe how this changes.

Also, the percent change in crack width compared to static conditions at initial load were determined at different load cycles.

These results are presented in Table 3.

CHAPTER V - CONCLUSIONS AND RECOMMENDATIONS FOR DESIGN

A total of eight beams with two different span to depth ratios were tested in fatigue. They all were simply-supported on steel rollers and all had steel reinforcement anchored at the ends to steel plates by welding.

Generally, fatigue failure may occur in the end anchorages preceded by bond failure, or due to cracking in the concrete leading to rupture of the compressed region, or due to rupture of the steel bar.

The conclusions obtained from these experiments can be divided into three parts and tabulated as follows:

General Conclusions

1. Long before failure, the external surface cracking will be observed. In fact, this was seen almost immediately after the first few load cycles.

2. The fatigue strength of concrete was dependent on the number of load cycles, stress range and the magnitude of stress.

3. No warning of impending failure in fatigue could be determined from the appearance.

4. The photoelastic coating is a valuable technique to monitor cracking in concrete.

5. The investigation on the effects of the number of load cycles on fatigue performance has confirmed the conclusion of other research workers that an increase in the number of cycles will increase the width and depth of the crack (10).

6. The following conclusion reached stated in Ref. 10 was not confirmed.

After a crack appears in the concrete, it will start to grow and

almost no new cracks will form. In our experiments several new cracks were observed as load cycles increased.

Design Type One (L/D = 3.75)

1. Fatigue failure was due to progressive internal micro-cracking, debonding and finally, separation of the steel from the end anchorages.

2. Special attention should be given to the end anchorages (the welded connection between the end plates and the steel bars).

Design Type Two (L/D = 10)

1. Bond failure under cyclic load was unimportant due to the method of end anchorages for the reinforcing steel.

2. Fatigue failure was initiated by complete penetration of a crack through the compressed region of the concrete.

For the future research, the following work could be considered for this type of beam.

1. Change the stress level and range of loading to see how these affect the fatigue life and mode of failure.

2. Determine the fatigue performance under different moisture conditions.

3. Determine if the age of the concrete at the time of initial loading affect on its fatigue strength.

4. Consider the effect of loading frequency on the fatigue life of reinforced concrete.

APPENDIX I

A. Calculation of Bond Stress

Flexural bond, which is the shearing stress produced over the steel contact area in the beam, can be calculated as

$$u = \frac{V}{\Sigma_o z}$$

V = total shear at the section under consideration

Σ_o = the sum of perimeters of all the bars at the section

z = moment arm at the section

If the bars used have no surface deformation, the bond will be produced by mechanical friction between the concrete and steel and by chemical adhesion. Bond strength between the natural roughness of the bar and concrete is very low and the beam will collapse when the bar is pulled through the concrete. In this case, end anchorage is recommended.

Such a beam with end anchorage will not collapse even if the bond is broken over the entire length of bars. The reason is that the sections of compressed concrete will act as a tied-arch which is shown in Fig. 16.

An increased width of crack and larger deflection is the result of the total steel elongation in such a beam. This situation can be improved by using the deformed bar, and by using a hook or end anchorage plate which will reduce the crack and the deflections.

The results of bond failure generally will split the concrete along the bar in two directions, either in the horizontal plane or in the vertical plane.

The ultimate average bond force per inch of length of bar was found approximately as (12)

$$U_u' = 35\sqrt{f_c'}$$

which can be written as bond stress per sq-in. of contact area:

$$U_u' = \frac{U_u'}{\Sigma_o} = 11 \frac{\sqrt{f_c'}}{\Sigma d_b} \quad .$$

The development length can be calculated by using the above as

$$\ell_d = A_b f_s / U_u'$$

In order to ensure that the bar is securely anchored by bond to develop its maximum strength, ℓ_d can be calculated as

$$\ell_d = \frac{A_b f_y}{U_u'} = \frac{0.028\ A_b f_y}{\sqrt{f_c'}} \quad .$$

As Fig. 17 shows, if ℓ is larger than ℓ_d, no bond failure will occur.

B. Design Calculations for Beam Type One

$f_c' = 5000$ psi

$f_y = 40{,}000$ psi

$\rho = 0.0582$

$n = 7$

$b = 3$ in.

$A_s = 0.611$ sq-in. (2 No. 5 bars)

$d = 3.5$ in.

$\rho n = 0.4073$

$L = 15$ in.

$f_r = 7.5\sqrt{5000} = 530$ psi

P @ center

$k = 0.583$

$kd = 2.04$ in.

$$I_{TR} = \frac{1}{3} b(kd)^3 + nA_s(d-kd)^2 = \frac{1}{3}(3)(2.04)^3 + 7(0.611)(3.5-2.04)^2$$

$$= 17.61 \text{ in}^4$$

$y_{top} = 2.04"$, $y_{bott} = 1.96"$

$$f = \frac{MC}{I}$$

If $f_c = 0.5\ f_c' = 2.5$ ksi

$$M = \frac{(17.61)(2.5)}{2.04} = 21.58^{K''}$$

$$P = 5.75^{K}$$

$$f_s = (7)\ \frac{21.58 \times 1.96}{17.61} = 16.8 \text{ ksi}$$

$$f_s = 42\%\ f_y$$

$$u = \frac{5.75/2 \times 1000}{(3.9)(1 - .583/3)3.5} = 261 \text{ psi}$$

A picture of the section is given in Fig. 2.

C. Design Calculations for Beam Type Two

Span = 15"	Bar size No. 2
Overall depth = 1.5"	D = 0.25"
Width = 3"	Cover = 0.175"
d = 1.2"	3 No. 2 used
$f_c' = 5000$ psi	$A_s = 0.147$ in.^{2}
$f_y = 40000$ psi	
n = 7	
$\rho = \frac{A_s}{bd} = \frac{0.147}{3x1.2} = 0.0408$	
$\rho n = 0.286$	j = .826
k = 0.522	
kd = 0.627"	

If,

$$f_c = 2.5 \text{ ksi}$$

$$M_c = \frac{1}{2}\ f_c\ kjd^2b \rightarrow M_c = 2.33^{K''}$$

$$M_s = f_s A_s jd \rightarrow f_s = 10.9 \text{ ksi}$$

$$P_{max} = \frac{4}{15''} (2.33 \text{ K}'') = 0.621^{K}$$

$$u = 132 \text{ psi}$$

$$V_c = \frac{V}{bjd} = 104 \text{ psi} \qquad \Sigma_o = 3 \times \frac{1}{4} \times \pi = 2.37$$

A picture of the section is given in Fig. 3.

APPENDIX II - NOTATION

A_b = Area of one bar

A_s = Total area of the steel bars

b = Width of specimen

C_c = Coefficient of sensitivity of photoelastic coating

D = Depth of specimen

D_n = Cycle dependent damage

D_t = Time dependent damage with a sustain load

d_b = Bar diameter

d = Distance of extreme compression fiber to centroid of tension reinforcement

f_y = Yield strength of steel, psi

f'_c = Compressive strength of concrete, psi

f_ϵ = Photoelastic coating fringe valve

H_c = Thickness of coating

I_{TR} = Transformed moment of inertia of beam

kd = Distance between line of C and T forces, inches

L = Length of specimen

ℓ_d = Development length of bar

M = Moment

n' = Number of applied cycles

n_o = Number of cycles to failure under pure fatigue condition

n = Modular ratio

p = The probability of specimen failure

P = Applied load

Q = Probability of failure of prototype at or before N cycles

t = Duration of loading under constant stress

t_u = Time of loading under constant stress level

u_1 = The ratio of width of the beam to the width of the test specimen

u = Flexural bond

U'_u = Ultimate average bond force per inch of length

V = Total shear

x = Maximum intensity of light

y = Intensity of light (amplitude) at any time

w = The circular frequency of the radiation

ρ_b = Balanced ratio

Σ_o = The sum of perimeters of all the bars

APPENDIX III - REFERENCES

1. Award, M.E. and Hilsdorf, H. K., "Strength and Deformation Characteristics of Plain Concrete Subjected to High Repeated and Sustained Loads," Fatigue of Concrete, ACI Publication No. SP-41, American Concrete Institute, Detroit, Michigan, 1974.

2. ACI Committee 215, "Considerations for Design of Concrete Structures Subjected to Fatigue Loading," ACI Journal, Vol. 71, No. 3, March 1974.

3. Dev B. Batchelor and Hewitt, E. B., "Are Composite Bridge Slabs Too Conservatively Designed? -- Fatigue Studies," Fatigue of Concrete, ACI Publication No. SP-41, American Concrete Institute, Detroit, Michigan, 1974.

4. Dove, R. C. and Adams, H. P., Experimental Stress Analysis and Motion Measurement, Charles E. Merrill Books, Inc., Columbus, Ohio, 1964.

5. Ople, S. F. and Hulsbos, L. C., "Probable Fatigue Life of Plain Concrete With Stress Gradient," ACI Journal, Vol. 63, No. 1, January 1966.

6. Raithby, K. D. and Galloway, J. W., "Effects of Moisture Condition, Age, and Rate of Loading of Fatigue of Plain Concrete," Fatigue of Concrete, ACI Publication No. SP-41, American Concrete Institute, Detroit, Michigan, 1974.

7. Shah, S. P. and Chandra, S., "Fracture of Concrete Subjected to Cyclic and Sustained Loading," ACI Journal, Vol. 67, No. 10, October 1970.

8. Swartz, Stuart E., Hu, K. K., Jones, Gary L., "Compliance Monitoring of Crack Growth in Concrete," Journal of the Engineering Mechanics Division, ASCE, Vol. 104, No. EM4, August 1978.

9. Venuti, William J., "A Statistical Approach to the Analysis of Fatigue Failure of Prestressed Concrete Beams," ACI Journal, Vol. 62, No. 11, November 1965.

10. Walls, J. C., Sanders, W. W., Munse, W. H., "Fatigue Behavior of Butt-welded Reinforcing Bars in Reinforced Concrete Beams," ACI Journal, Vol. 62, No. 2, February 1965.

11. Zandman, F., Redner, S., Dally, James W., Photoelastic Coatings, SESA Monograph No. 1, Society for Experimental Stress Analysis, Westport, Conn., 1977.

12. Winter, George, Nilson, H. Arthur, Design of Concrete Structures, McGraw-Hill, Inc., New York, N.Y., 1972.

APPENDIX IV - TABLES AND FIGURES

TABLE 1: Compressive Cylinder Strength

No.	Failure Load lb.	Failure Stress psi.
1	33250	4703
2	33000	4668
3	32400	4583
4	31100	4399
5	30900	4371
6	29237	4135

a. 3 in. x 6 in. cylinders, area = 7.07 $in.^2$

b. Average stress, f'_c = 4476 psi.

TABLE 2: Load and Stresses for the Test Specimens

Specimen No.	Type	Loads-lb.		Concrete Stress		Steel Stress		Cycle
		P-max.	Range	f_c-max. ksi	f_c-Range ksi	f_s-max. ksi	f_s-Range ksi	To Failure
1	I	5000	4000	2.17	1.74	10.88	8.71	93,000
2	I	5000	4000	2.17	1.74	10.88	8.71	112,000
3	I	5000	4000	2.17	1.74	10.88	8.71	179,000
4	I	5000	4000	2.17	1.74	10.88	8.71	--- *
5	I	5000	4000	2.17	1.74	10.88	8.71	324,000
6	I	5000	4000	2.17	1.74	10.88	8.71	389,000
7	II	600	600	2.42	2.42	15.45	15.45	4,830,000
8	II	800	600	3.22	2.42	20.6	15.45	

*Beam #4 failed under a sudden manner.

TABLE 3: Crack Size V Number of Cycles

Beam #7

No. of Cycles x 10^3	Maximum Crack Depth/Beam Depth	% Change in Crack Width
0	0.232	
25	0.344	5%
850	0.376	11%
1174	0.400	74%
2690	0.408	79%
3600	0.432	79%
4300	0.600	137%

These results are for the center crack under the point of load application.

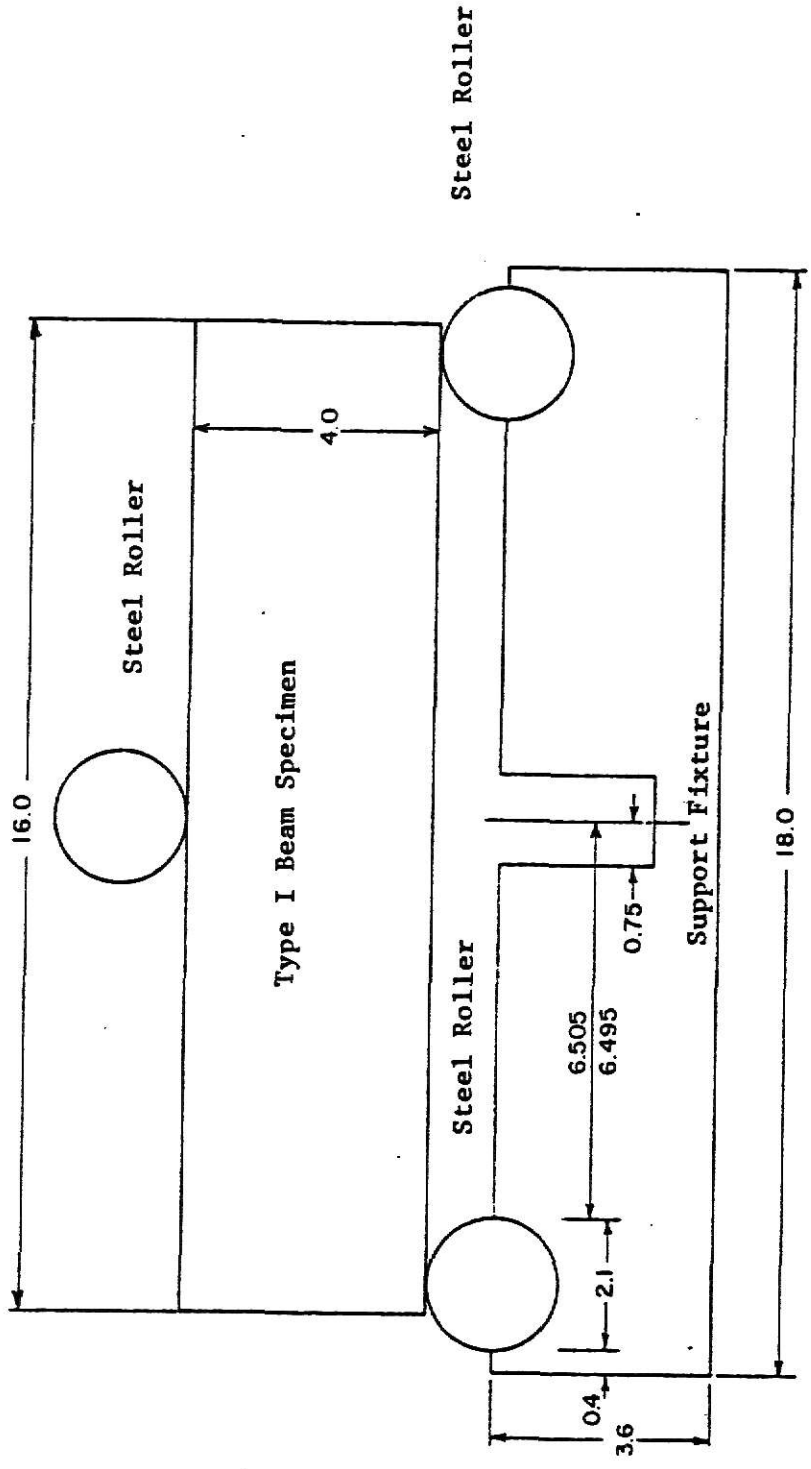

All dimensions in inches. 1 in. = 2.54 cm.

Fig. 1: Test Fixture and Specimen Dimension

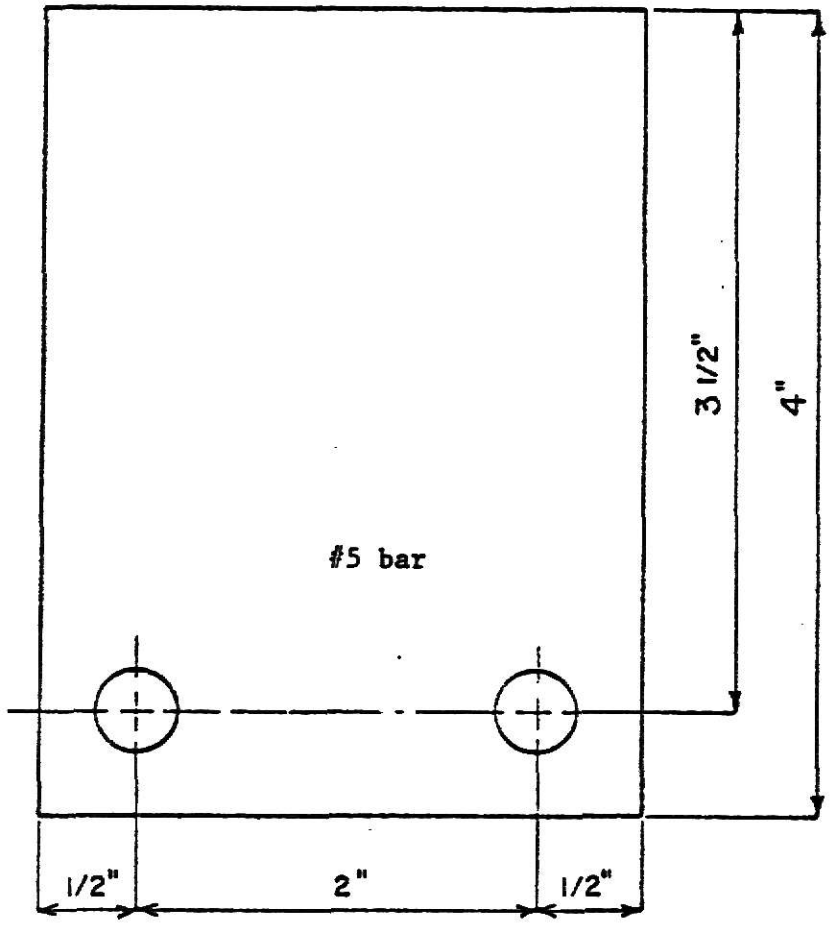

Fig. 2: Model Cross-Section of Type One

Fig. 2: Model Cross-Section of Type One

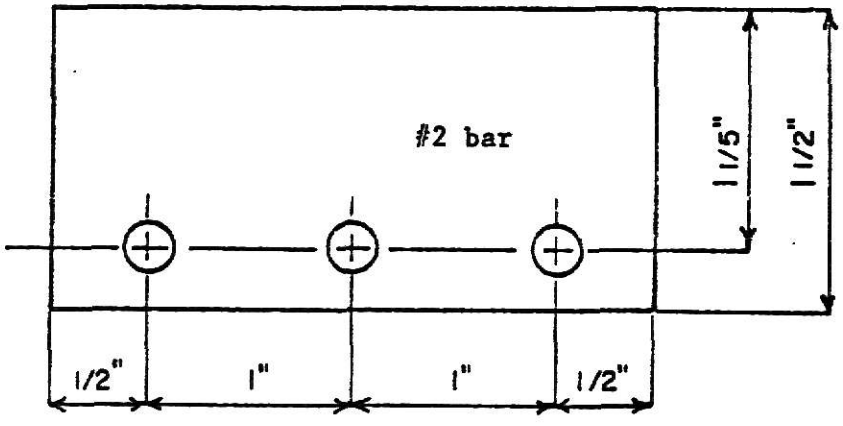

Fig. 3: Model Cross-Section of Type Two

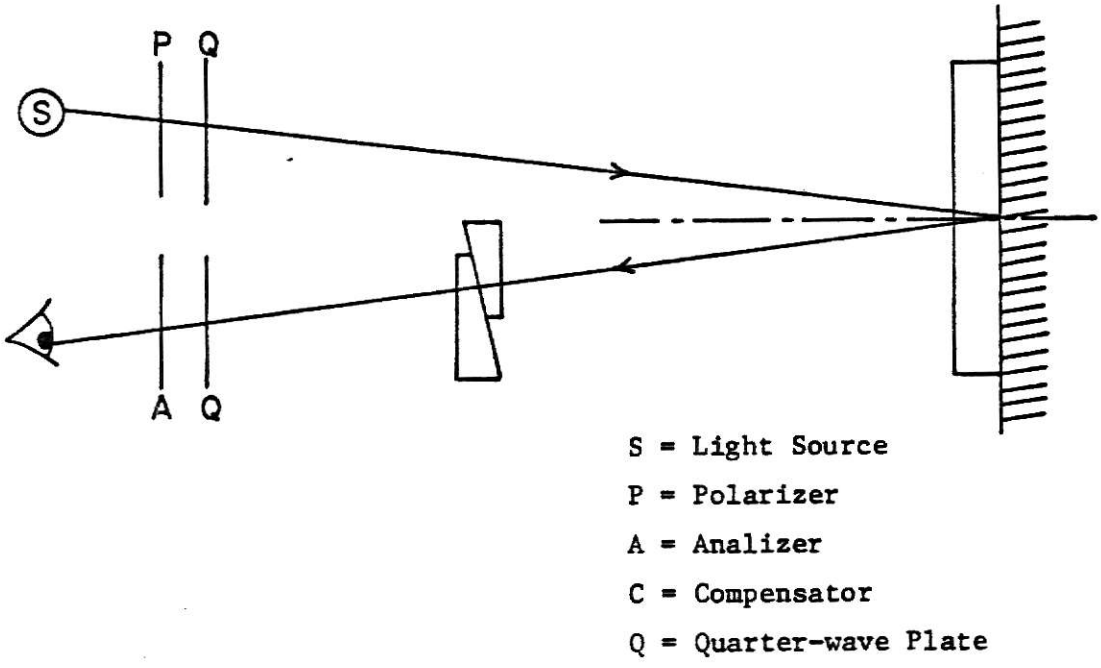

Fig. 4: Arrangements for a Reflection Polariscope

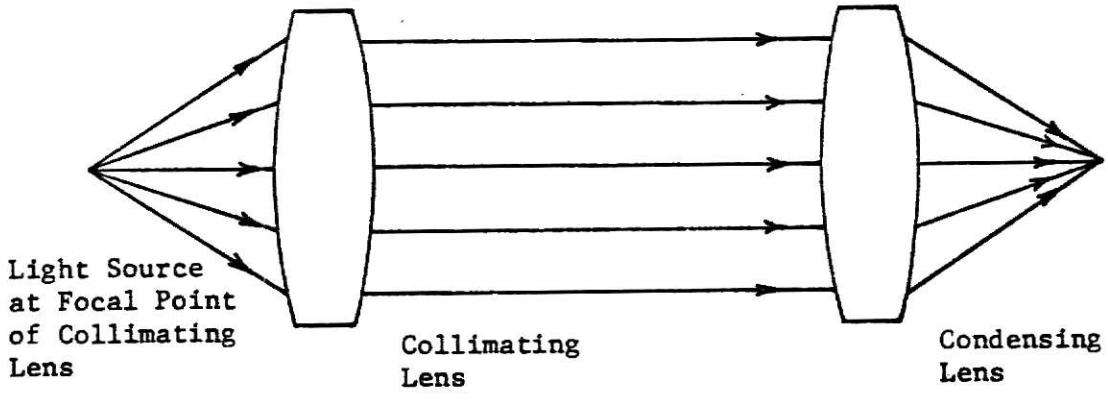

Fig. 5: Collimation of Light

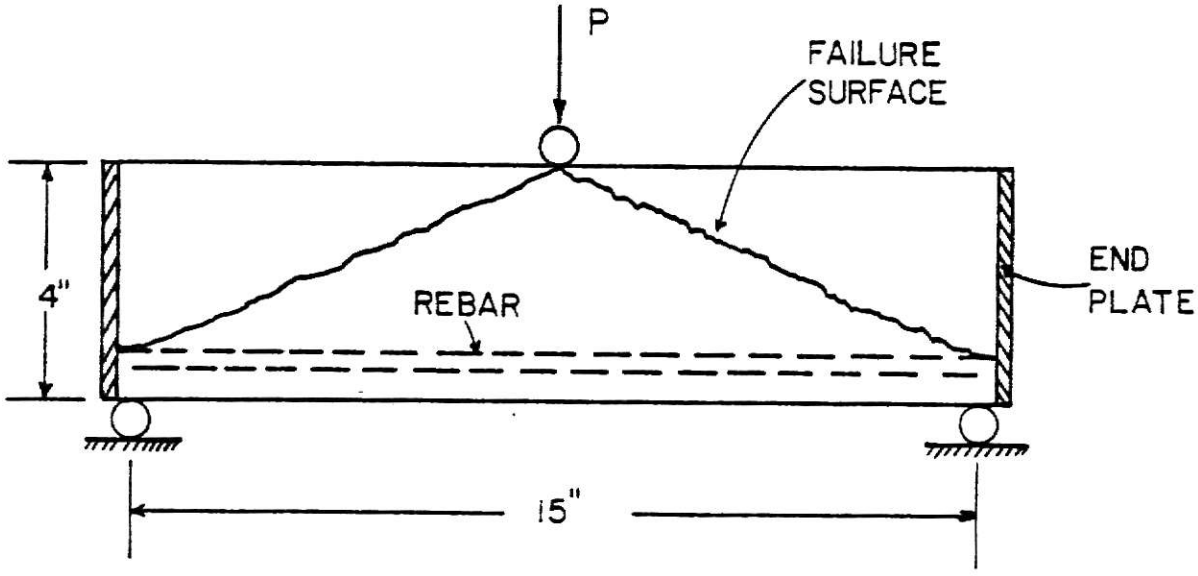

Fig. 6: Mode of Failure-Group One Beams

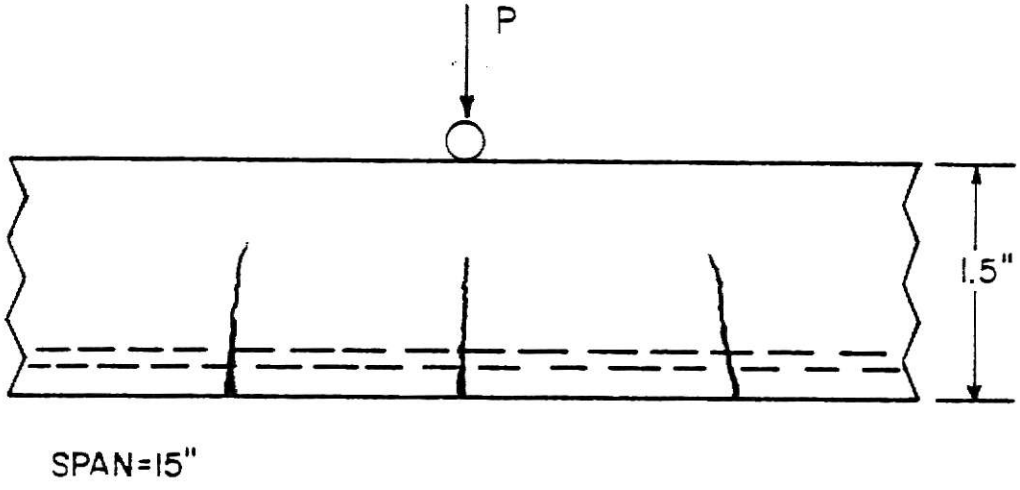

Fig. 7: Crack Pattern in Center-Group Two Beams

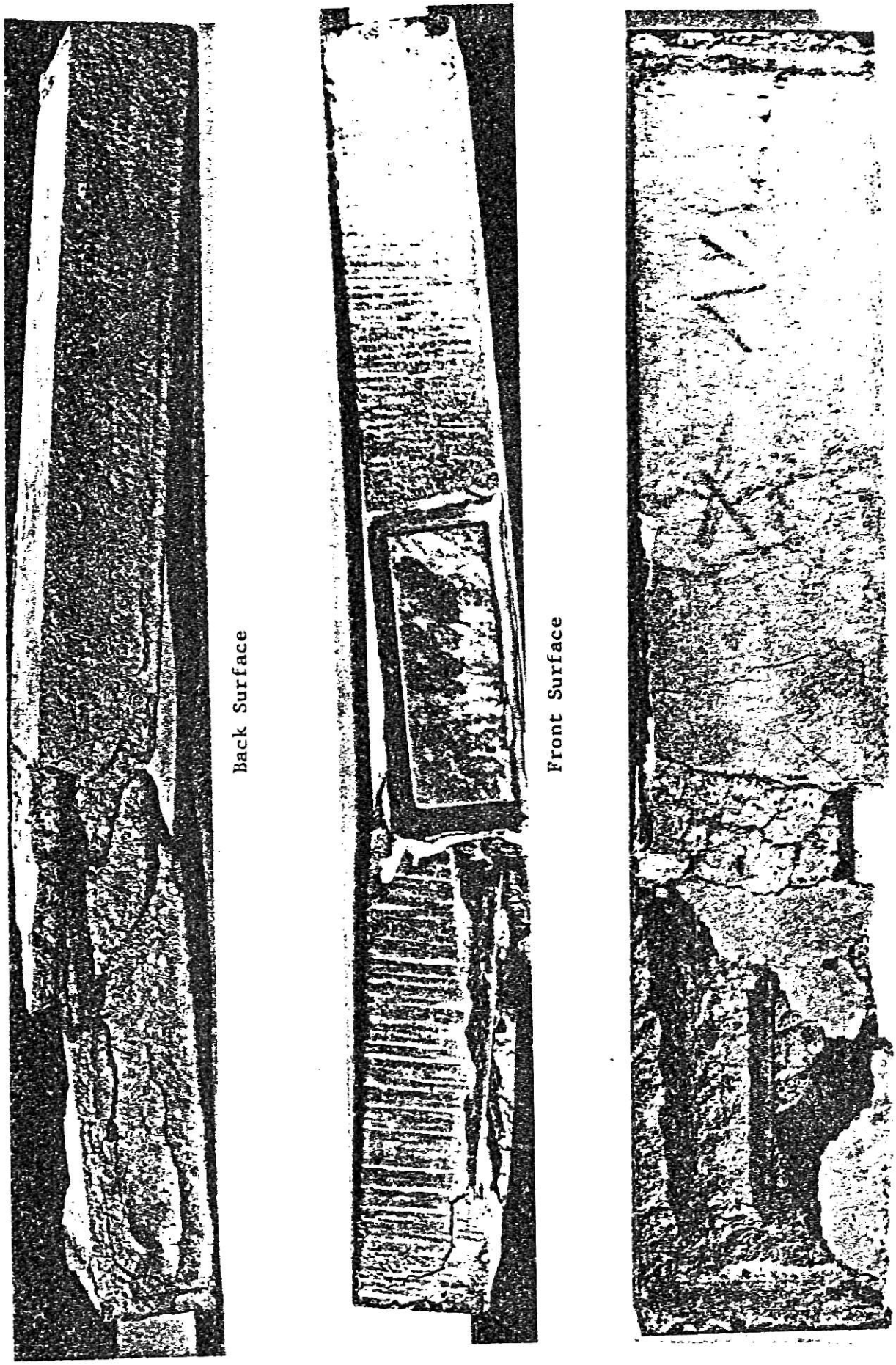

Fig. 8: Mode of Fallure, Group Two Beams

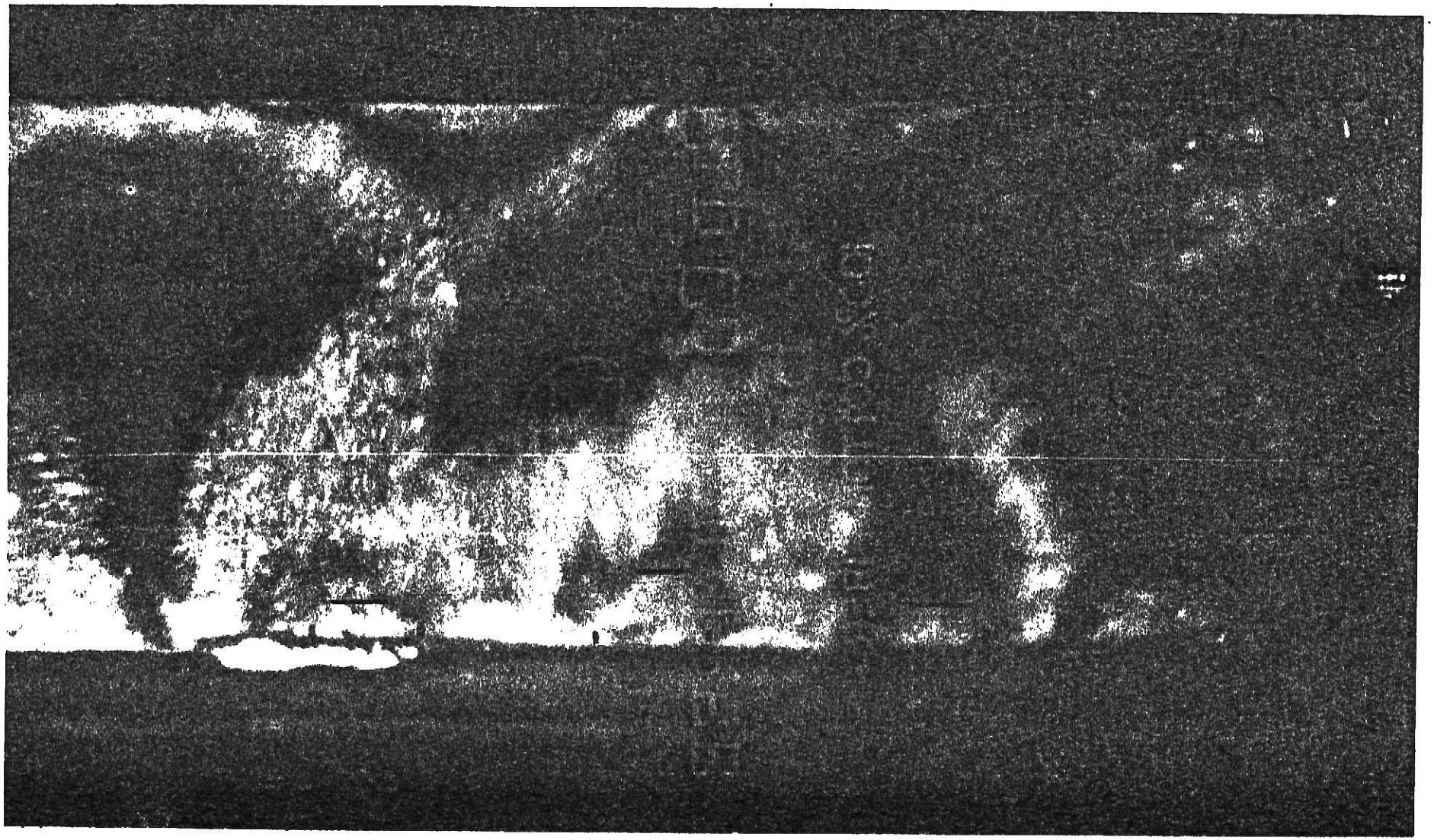

Fig. 9: Typical Crack Patterns Observed on Photoelastic Coating at About 0 Cycles.

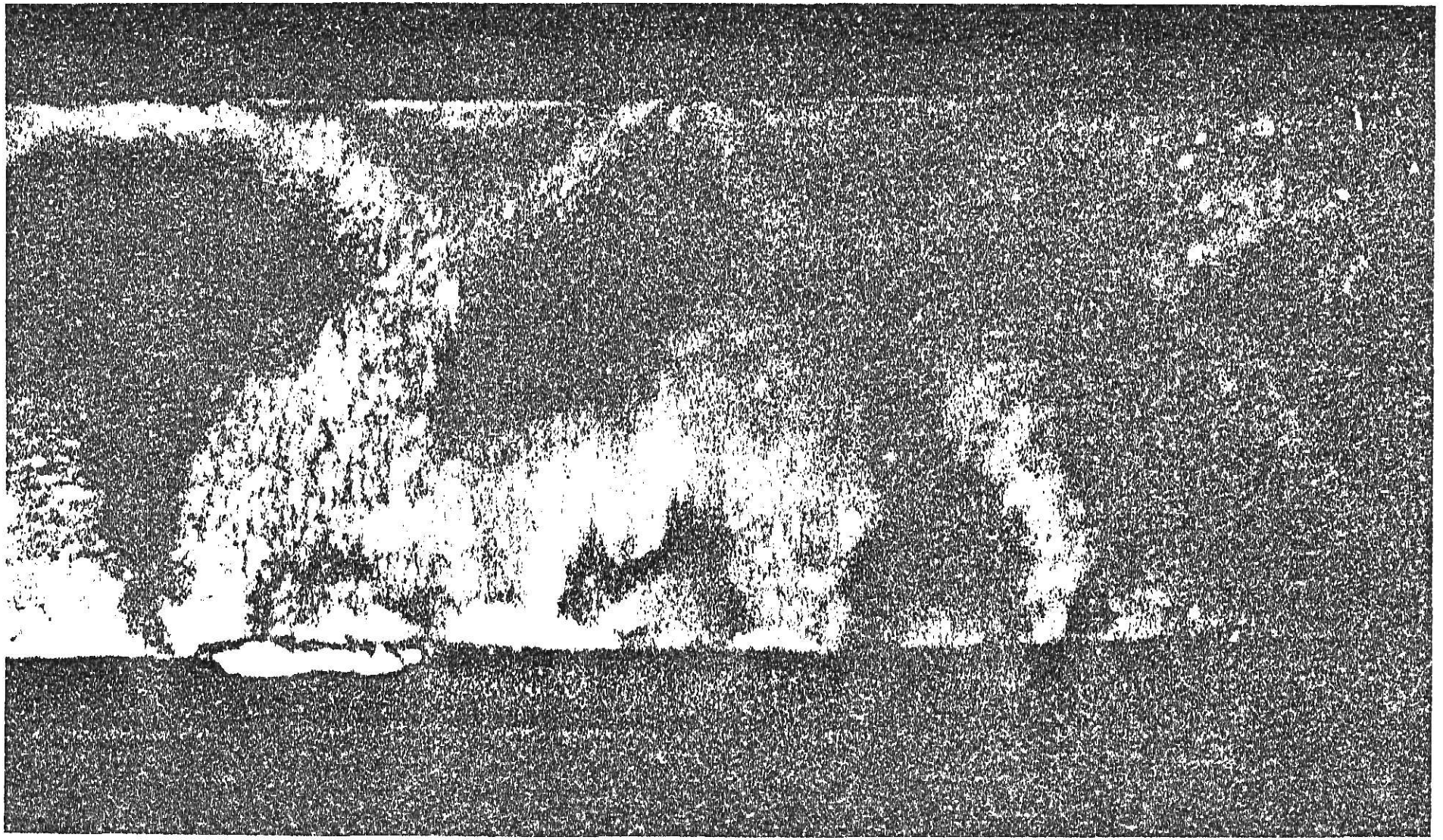

Fig. 10: Typical Crack Patterns Observed on Photoelastic Coating at About 25,000 Cycles

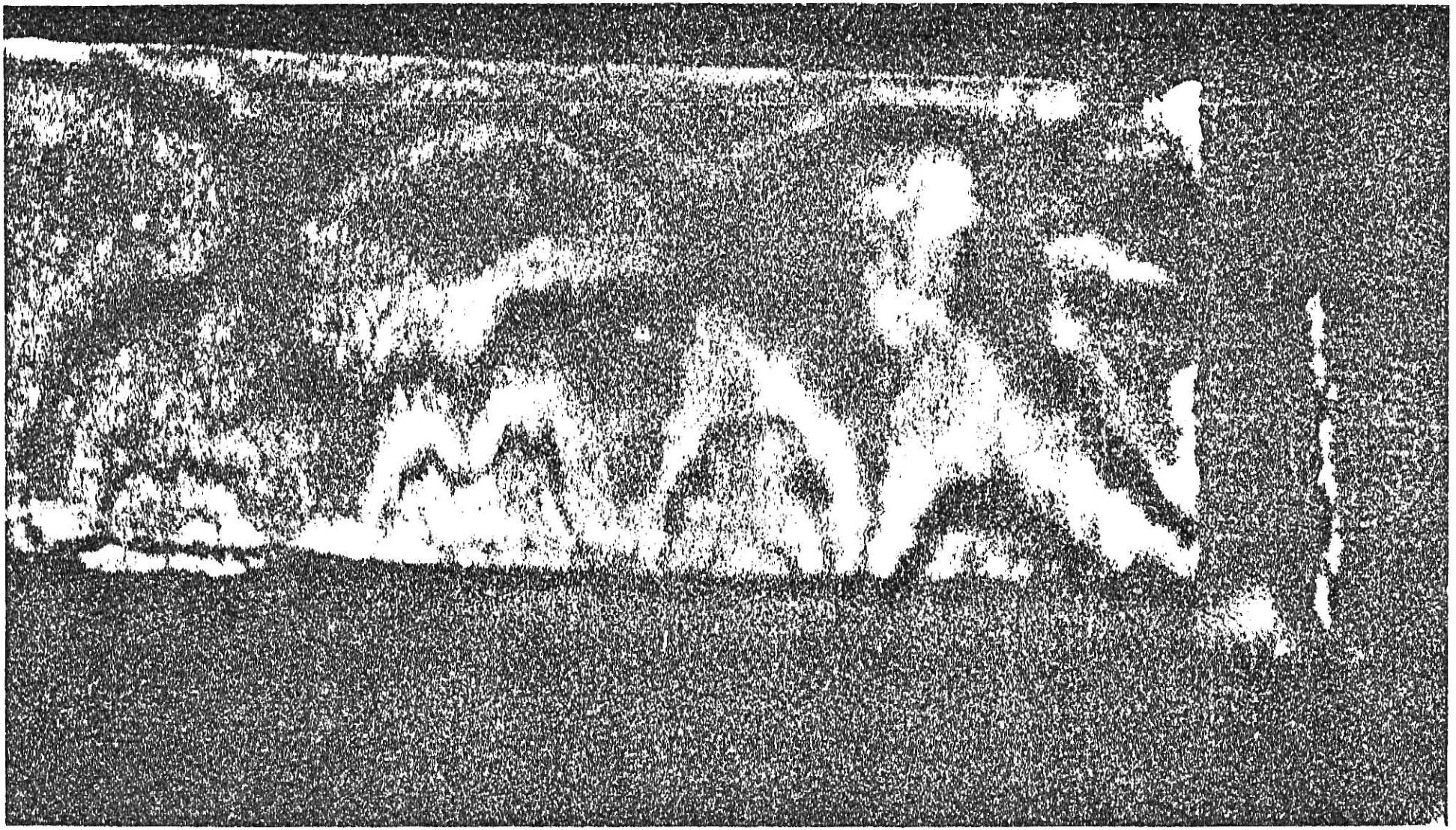

Fig. 11: Typical Crack Patterns Observed on Photoelastic Coating at About 850,000 Cycles

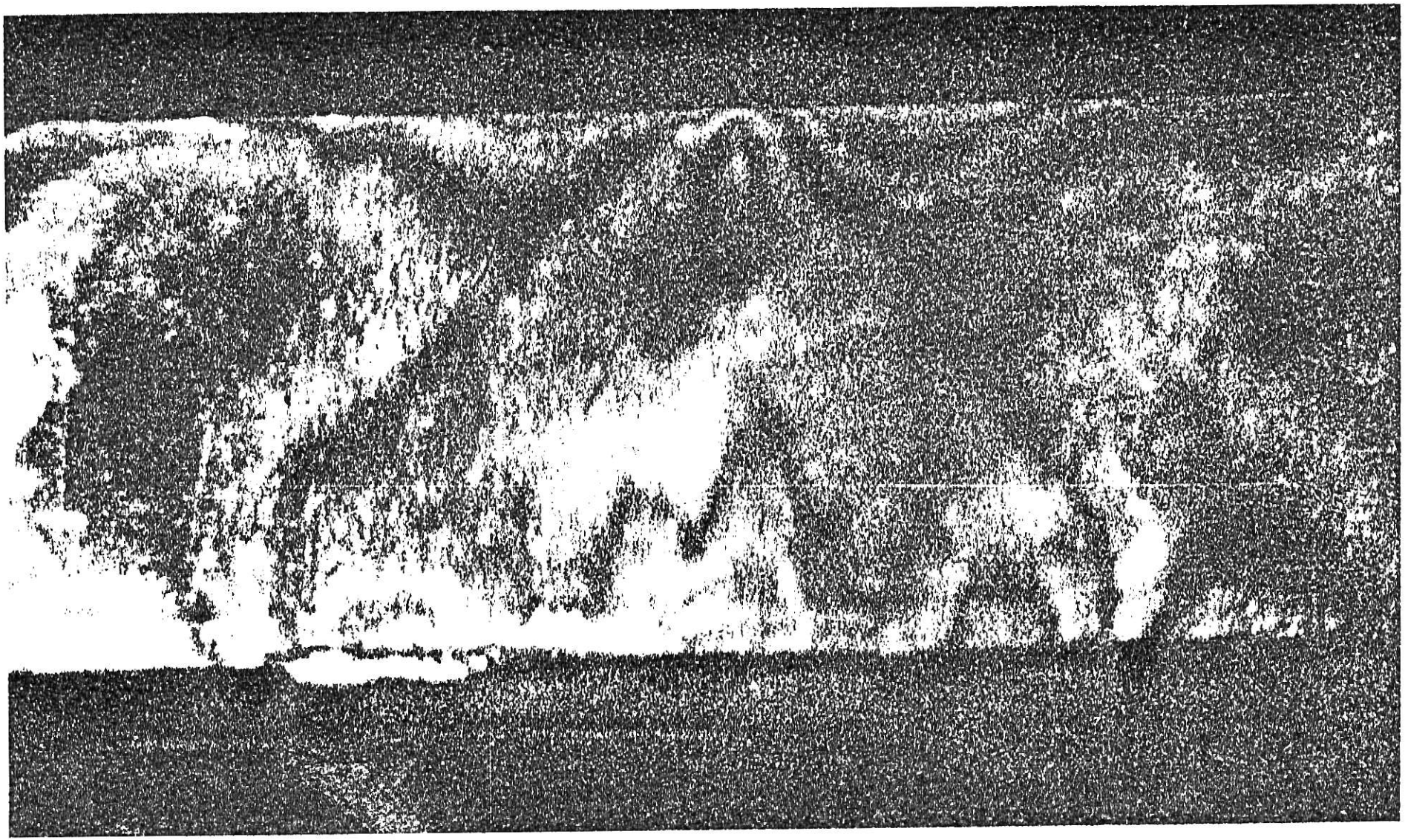

Fig. 12: Typical Crack Patterns Observed on Photoelastic Coating at About 1,174,000 Cycles

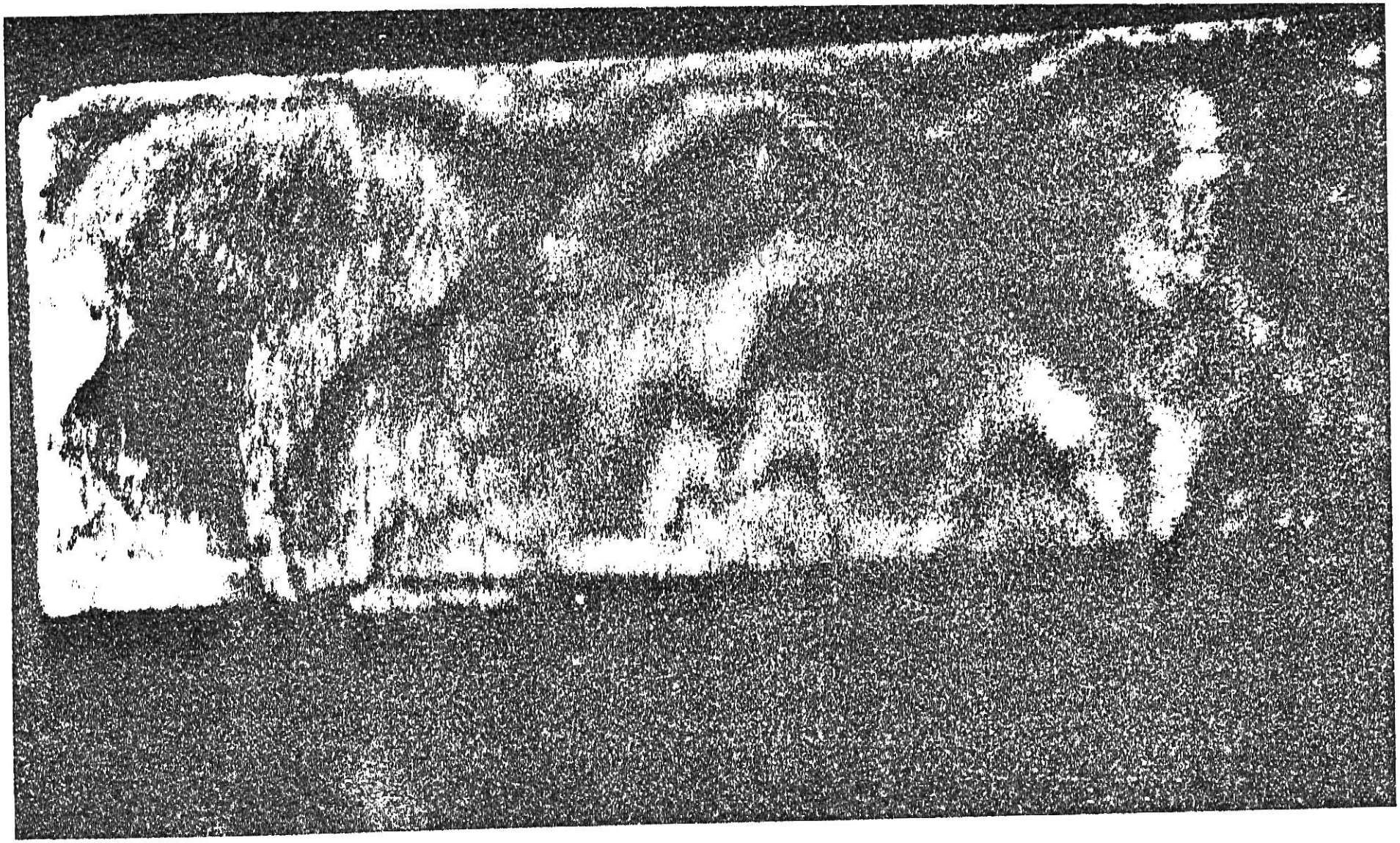

Fig. 13: Typical Crack Patterns Observed on Photoelastic Coating at About 2,690,000 Cycles

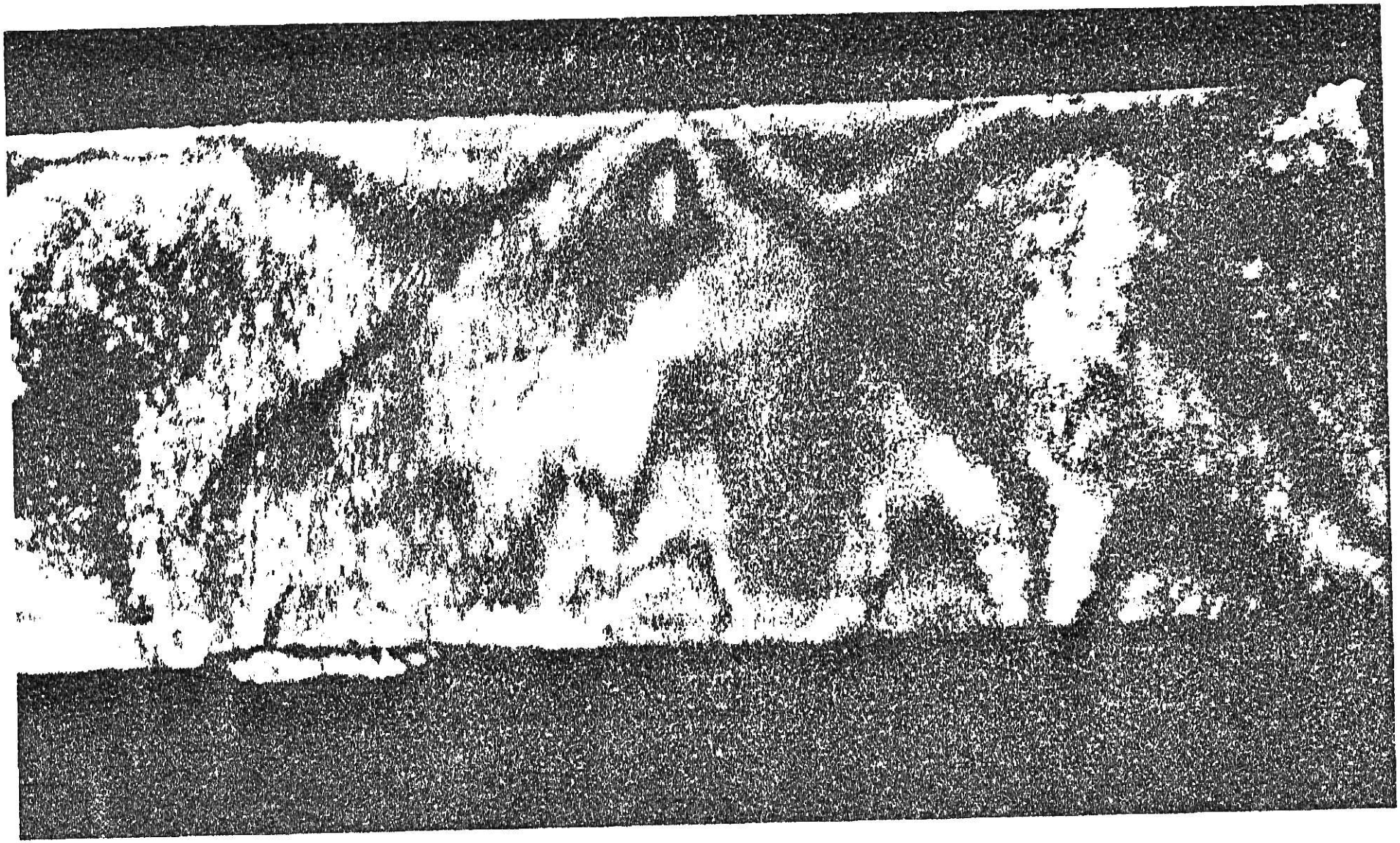

Fig. 14: Typical Crack Patterns Observed on Photoelastic Coating at About 3,600,000 Cycles

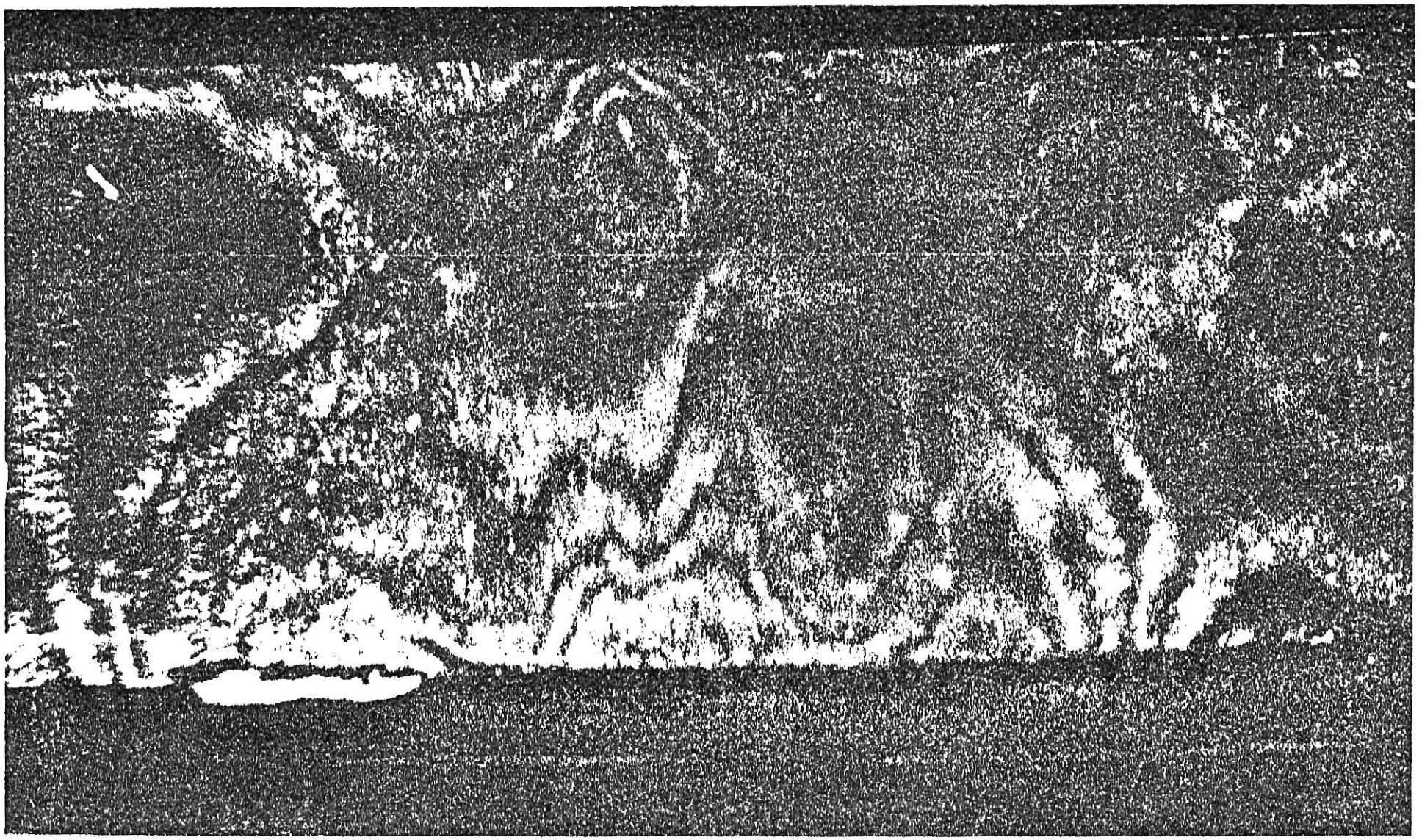

Fig. 15: Typical Crack Patterns Observed on Photoelastic Coating at About 4,300,000 Cycles

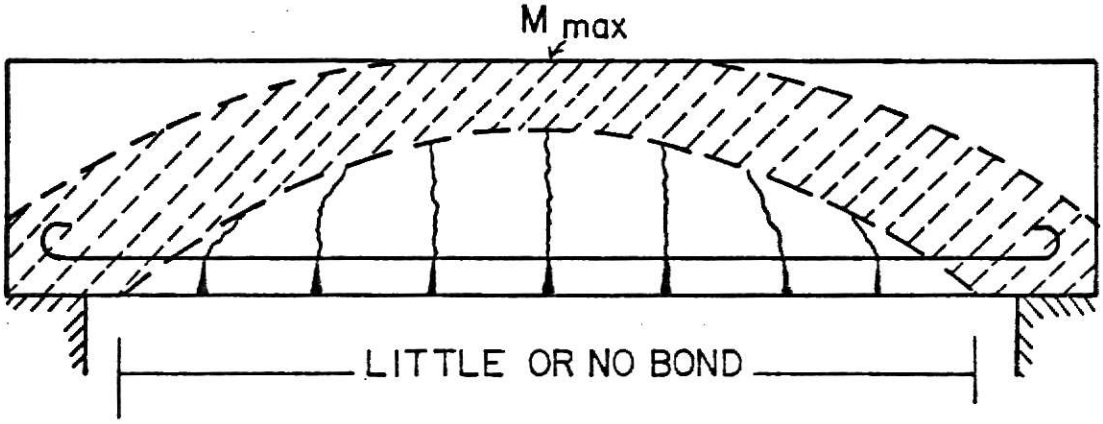

Fig. 16: Tied-Arch Action in Beam With Little or No Bond

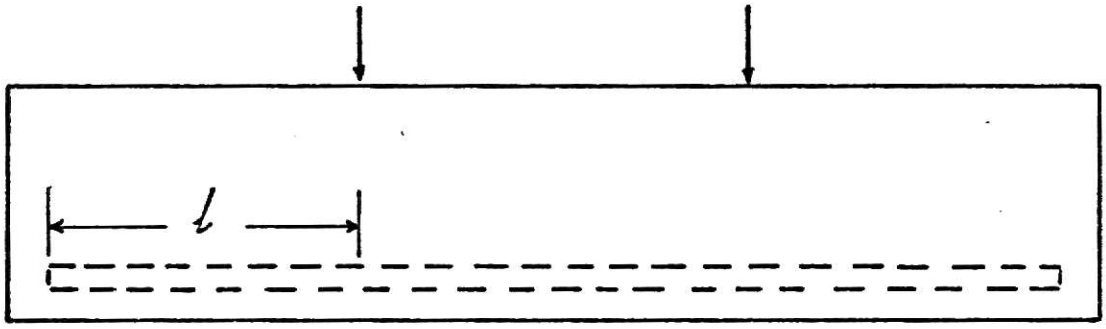

Fig. 17: Development Length

ACKNOWLEDGMENTS

The author is greatly indebted to his major professor, Dr. Stuart E. Swartz, for invaluable advice and guidance during his study at Kansas State University and carrying out this investigation.

Sincere thanks is also extended to Dr. Robert R. Snell, Head of the Department of Civil Engineering for his support. Appreciation is also due to the other committee members: Dr. Kuo-Kuang Hu, Dr. Leonard E. Fuller for their efforts in reviewing this report.

Special appreciation is also expressed to Russell L. Gillespie, Civil Engineering Laboratory Technician, for his help in using the facilities.

FATIGUE OF SMALL REINFORCED CONCRETE BEAMS WITH END-ANCHORED REINFORCEMENT

by

ABOLFAZL NOORY-KOOPAEE

B.S.C.E., Kansas State University, 1978

AN ABSTRACT OF A MASTER'S REPORT

submitted in partial fulfillment of the

requirements for the degree

MASTER OF SCIENCE

Department of Civil Engineering

Kansas State University

Manhattan, Kansas

1978

ABSTRACT

The objective of this report is to present results of tests on reinforced concrete beams subjected to repeated loads.

Crack growth vs. load cycles is shown by use of the photoelastic coating method. A further objective was to observe the mode of failure in beams with different depth to span ratios. All beams tested were reinforced with steel bars anchored at their ends to steel plates by welding.

The suitability of the photoelastic coating technique to monitor cracking in concrete was evaluated and found to be acceptable.

The following conclusions were reached from the tests presented in this report:

1. Fatigue failure in these concrete beams is due to progressive internal micro-cracking and/or failure of the end anchorages.

2. Special attention should be given to the welded connection between the end plates and the steel bars.

3. Bond failure under cyclic load is unimportant due to the method of end anchorages for the reinforcing steel.

4. The fatigue strength of concrete should be considered to depend on the number of loading cycles, the stress range and the magnitude of stress.

5. No warning of impending failure in fatigue could be determined from the opening and closing of the concrete cracks, although these become quite enhanced as the number of load repetitions increased.